Pharmacokinetics-pharmacodynamics and antitumor activity of mercaptoacetamide-based histone deacetylase inhibitors

Zacharoula Konsoula,[1] Hong Cao,[2] Alfredo Velena,[1] and Mira Jung[1]

Departments of [1]Radiation Medicine and [2]Biochemistry and Molecular and Cellular Biology, Lombardi Comprehensive Cancer Center Georgetown University Medical Center, Washington, District of Columbia

Abstract

Structurally diverse histone deacetylase inhibitors (HDACI) have emerged as chemotherapeutic agents. Here, we report the first mercaptoacetamide HDACIs (coded 6MAQH and 5MABMA) for use in treatment against prostate cancer cells *in vitro* and *in vivo* and correlate their plasma pharmacokinetics and tissue-pharmacodynamics with tumor sensitivity. HDACIs were assessed for *in vitro* microsomal stability and growth inhibition against prostate cancer and nonmalignant cells. Antitumor activity was determined following i.p. administration of 6MAQH and 5MABMA (0.5 and 5 mg/Kg) using mice bearing PC3 tumor xenografts ($n = 10$). The plasma pharmacokinetics of 6MAQH and 5MABMA and their effects on the acetylation of histone H4 in tissues were determined in athymic mice. Both HDACIs significantly inhibited the growth of cancer cells while exerting limited effect on nonmalignant cells. They exhibited stability in human, dog, and rat microsomes [$t_{1/2\ (min)} = 83$, 72, and 66 for 6MAQH and 68, 43, and 70 for 5MABMA, respectively]. Both HDACIs (0.5 mg/Kg) led to tumor regression ($P < 0.01$), which was sustained for at least 60 days. *In vivo* data show favorable plasma pharmacokinetics with the area under the curve of 4.97 ± 0.6 μmol/L × h for 6MAQH and 4.23 ± 0.43 μmol/L × h for 5MABMA. The clearance rates for 6MAQH and 5MABMA were 4.05 ± 0.15 and 4.87 ± 0.2 L/h, whereas the half-lives were 2.2 ± 0.33 and 1.98 ± 0.21 h, respectively. Both HDACIs markedly enhanced the acetylation of histone H4 within 30 minutes in tissues, including the brain, liver, and spleen. Taken together, the results provide a rationale for further investigation of these mercaptoacetamide HDACIs as potent anticancer agents. [Mol Cancer Ther 2009;8(10):2844–51]

Introduction

Prostate cancer is the most common male malignancy within the developed world and the second leading cause of cancer in American men (1). Over the last decade, improvements in the detection and treatment of prostate tumors have extended the lives of cancer patients; however, the incidence and recurrence rates of the disease still remain high (2).

Histone acetylation, one of the major players mediating epigenetic modifications, is determined by the antagonistic actions of histone acetyltransferases and histone deacetylases (HDAC; refs. 3, 4). The increased attention on inhibiting the HDACs as targets for cancer therapy stems from their well-established ability to modify several cellular functions that are deregulated in cancer cells. Attenuation of HDACs often leads to cellular differentiation, growth arrest, and apoptosis in a broad spectrum of tumor cells and *in vivo* (5–7). Several HDAC inhibitors such as vorinostat [Zolinza, suberoylanilide hydroxamic acid (SAHA); ref. 8], phenylbutyrate (9), MS-275 (10), and depsipeptide (11) have shown potent antitumor characteristics and are currently in phase I and II clinical trials.

Nevertheless, a vorinostat known as SAHA, which was recently approved by the Food and Drug Administration for the treatment of cutaneous T-cell lymphoma, is not an ideal drug due to its low solubility and permeability classification (class IV), according to the Biopharmaceutical Classification System, and because of its short half-life in clinical trials (half-life of 120 minutes for oral administration versus 40 minutes for i.v.; ref. 12). Moreover, HDACIs with substantially longer half-lives, such as MS-275 with a half-life of up to 80 hours, display higher toxicity profiles (10). Additionally, valproic acid binds to serum proteins (up to 90% of the absorbed drug) and exhibits low potency (7).

In an earlier report (13), we examined the physicochemical properties of two mercaptoacetamide-based HDACIs (6MAQH and 5MABMA; refs. 13, 14) and compared them to SAHA. The two compounds exhibited favorable *in vitro* plasma stability, permeability, solubility, and lipophilicity (log *D*) compared with SAHA. The objective of the present work is to extend and translate our investigations of the *in vitro* properties of mercaptoacetamide-based HDACIs into *in vivo* studies.

Received 4/7/09; revised 7/8/09; accepted 8/10/09; published OnlineFirst 9/29/09.

Grant support: W81XWH-04-1-0170 (M. Jung), U.S. Army Medical Research and Materiel Command.

The costs of publication of this article were defrayed in part by the payment of page charges. This article must therefore be hereby marked *advertisement* in accordance with 18 U.S.C. Section 1734 solely to indicate this fact.

Note: Supplementary materials for this article are available at Molecular Cancer Therapeutics Online (http://mct.aacrjournals.org/).

Requests for reprints: Mira Jung, Division of Radiation Biology, Department of Radiation Medicine, The Research Building, Room E-211, Georgetown University School of Medicine, Box 571482, 3970 Reservoir Road, Northwest, Washington, DC 20057-1482. Phone: 202-687-8352; Fax: 202-687-7529. E-mail: jungm@georgetown.edu

doi:10.1158/1535-7163.MCT-09-0629

Materials and Methods

Chemicals and Reagents

Cell culture supplies were purchased from Invitrogen. Chemicals (>99.9% purity) were obtained from Sigma-Aldrich Chemicals. Pooled liver microsomes of human, dog, and rat were purchased from BD Biosciences. Antibodies were purchased from Millipore. The mercaptoacetamide-based HDACIs (6MAQH and 5MABMA) have been patented by Georgetown University and were prepared by Gene Therapy Pharmaceutics.

Cells and Culture Conditions

Prostate cancer cells PC3 and LNCaP (Tissue Culture Shared Resources of the Lombardi Comprehensive Cancer Center) and nonmalignant prostate epithelial cells RWPE-1 and 267-B1 (National Cancer Institute, NIH) were maintained in RPMI 1640 culture medium supplemented with fetal bovine serum (10% v/v), L-glutamine (1 mmol/L), and antibiotics [streptomycin (100 mg/mL)/penicillin (100 U/mL)] at 37°C in an atmosphere of 5% CO_2.

Cell Proliferation Assay

Proliferation was measured by MTT assay (15) as previously described (16, 17). Briefly, cells were plated at 5×10^3 cells per well in 96-well plates in 100-μL medium and allowed to adhere to the plastic for 24 h. The compounds were dissolved in DMSO and diluted directly into the culture medium when required. The total concentration of DMSO in the medium did not exceed 0.5% (v/v) during treatments. The compounds were then added at seven different concentrations in quadruplicate wells and incubated at 37°C for 72, 96 h, and 7 d. Control groups consisting of cells in media (without compound) were processed identically. In the last hour of incubation, 10 μL of 5 mg/mL MTT were added and the cells were incubated at 37°C for 1 h, followed by the addition of 100 μL DMSO to solubilize the MTT. The same plate containing additional wells with media and chemicals only (without cells) was processed in parallel as a reference blank to test for chemically induced MTT reduction. Plates were read at a wavelength of 550 nm on a plate reader. Cell viability is expressed as a percentage of the control groups. Inhibitory concentration 50% (IC_{50}) values and the mean value of IC_{50} were calculated graphically (GraphPad Software, Inc.). Results are the mean of at least three determinations.

In vitro Metabolic Stability Studies

In vitro metabolic stability experiments were conducted in human, dog, and rat liver microsomes. The test compounds were prepared in PBS (pH 7.4) containing 0.5% DMSO. The incubation mixtures of 6MAQH and 5MABMA with liver microsomes consisted of PBS (final volume of 1.5 mL), microsomes (1 mg/mL), and 1 mmol/L of NADPH regenerating system. The reaction mixtures were done in triplicates and preincubated at 37°C for 10 min. The metabolism reactions were initiated by the addition of 5 μmol/L of the test compound to the incubation mixture. At time intervals of 5, 15, 30, 45, and 60 min, 50 μL aliquot of the reaction mixture were quenched using 150 μL of acetonitrile. The samples were centrifuged at 2,000 × *g* for 15 min at 4°C, and the supernatants were analyzed by liquid chromatography-mass spectrometry (LCMS). Negative controls were prepared by incubating reactions that excluded either the microsomes or the compounds from the mixture. Metabolic stability was assessed by monitoring the disappearance of the parent compound over the incubation period. Values in figures are expressed as percentages of the parent compound remaining. All incubations were done thrice and the mean values are presented.

In addition, *in vitro* half-lives were calculated using the expression $t_{1/2} = 0.693/b$, where b is the slope found in the linear fit of the natural logarithm of the fraction remaining between the parent compound versus incubation time.

Animals

Male athymic nude mice (*Foxn1*^{nu}) weighing 18 to 22 grams (ages 8–10 wk) were purchased from Taconic. The mice were maintained under specific pathogen-free conditions and provided with sterile food and water *ad libitum*. All studies were approved by the Institutional Animal Care and Use Committee of Georgetown University. The mice were allowed to acclimatize for at least 5 d before beginning the study.

Maximum Tolerated Dose

Male athymic nude mice were given increasing doses (0.5, 5, 10, 50, 100, 200, 300, 400 mg/Kg) of the compounds i.p. Dosing solutions were prepared by dissolving 6MAQH and 5MABMA in 0.5% (v/v) DMSO in normal saline. After 4 h of treatment, the mice were euthanized. Tissues were removed from each animal and were immediately either homogenized in cold lysis buffer or snap-frozen in liquid nitrogen and stored at −80°C. For pharmacodynamic profiling, three mice were sacrificed per dose, per compound.

In vivo Tumor Growth

To generate tumor xenografts, PC3 cells (5×10^6) were transplanted s.c. on both flanks of male nude athymic mice. When tumors reached a volume of ~100 mm^3, the mice were randomized into treatment and control groups (n = 10 mice/group). The compounds were freshly prepared for injection each day in 0.5% (v/v) DMSO in normal saline. The 6MAQH and 5MABMA were administered i.p., at a single daily dose of 0.5 mg/Kg, 5 d a week for 2 weeks. Control mice were treated with the vehicle alone. Tumor size was measured at regular (twice a week) intervals, and their volume was calculated by the following formula: A (length) × B (width) × C (height) × 1/2. All measurements were recorded in millimeters. Antitumor activity was determined by comparing the volumes of treated and control groups. The percentage change in tumor volume from the baseline was used to assess the response to treatment. Tumor volume was monitored up to 60 d. The body weight of control and treated mice was also measured at weekly intervals as an indicator of any toxicity that might be associated with the use of these compounds.

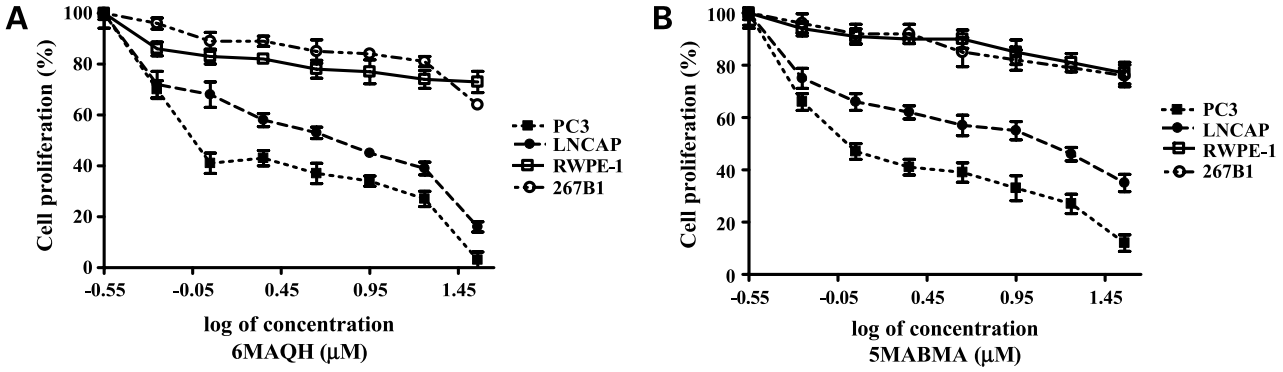

Figure 1. The effect of mercaptoacetamide-based HDACI compounds (**A**) 6MAQH and (**B**) 5MABMA on cell proliferation. The human prostate cancer PC-3 and LNCaP and nonmalignant 267-B1 and RWPE-1 epithelial cells were untreated or treated with indicated doses of HDACIs for 72 h. Cell viability was determined by MTT assay. Three independent experiments were done in triplicates; *points,* mean from a representative triplicate experiment; *bars,* SEM.

Pharmacokinetic-Pharmacodynamic Relationships in Nude Athymic Mice

6MAQH and 5MABMA, at the maximum tolerated dose (400 mg/Kg), were administered i.p. to nude athymic mice. The compounds were prepared in 0.5% (v/v) DMSO in normal saline. Mice were randomized into either a control or treatment group. For each time point, three mice were sacrificed. Blood was collected at various time points (0, 1, 2, 4, and 6 h after compound administration) by cardiac puncture under anesthesia, transferred to microcentrifuge tubes, and centrifuged at 15,000 × *g* for 5 min to obtain plasma. Plasma (100 μL) was then extracted with three volumes of acetonitrile, centrifuged at 2,000 × *g* for 15 min, and the resulting supernatants were analyzed by LCMS. Plasma concentrations were extrapolated from standard curves constructed by linear regression. In addition, tissues were rapidly dissected and snap frozen in liquid nitrogen. Samples were stored −80°C for Western blot analysis.

Detection of Acetylation of Histone H4 in Tissues

Tissues were thawed on ice and homogenized in a lysis buffer containing 31.5 mmol/L Tris-HCl (pH 7.4), 2 mmol/L EDTA (pH 7.4), 2 mmol/L EGTA (pH 7.4), 6 mmol/L mercaptoethanol, 10 μg/mL leupeptin, 2 μg/mL aprotinin, and 1% NP40. The homogenates were sonicated and centrifuged at 15,000 × *g* for 30 min at 4°C, and the pellets were discarded. The protein concentrations of the supernatants were determined by the Bradford assay. The samples were then treated with Laemmli sample buffer, denatured by boiling for 5 min, and subjected to SDS-PAGE. The separated proteins were transferred to polyvinylidene difluiride membrane and the nonspecific binding sites were blocked by incubation with 5% nonfat dry milk for 1 h at room temperature. The membrane was then incubated with polyclonal rabbit antibody against acetylated histone H4 (Lys5, 8, 12, and 16; Upstate, Inc.) overnight at 4°C. The Histone H1 antibody was used as a loading control. The immune-reactive bands were detected by enhanced chemiluminescence (Amersham Biosciences).

Pharmacokinetic Calculations

Pharmacokinetic analysis was determined using noncompartmental methods. The maximum measured plasma concentrations (C_{max}) and the time of C_{max} (t_{max}) were derived directly from the data. The area under the curve (AUC) was calculated using the log-linear trapezoidal method rule up to the last data point and was extrapolated to infinity with the following formula: C_{last}/β, where C_{last} is the last measured concentration time point. The elimination half-life was calculated with the equation $t_{1/2} = 0.693/\beta$, where β is the terminal rate constant. The clearance (Cl = dose/AUC) rate was also evaluated.

Analytic Procedure

For samples generated in the *in vitro* and *in vivo* studies, quantitative analysis was conducted using LCMS as previously described (13, 18). LC was done using a Shimadzu LC-20AD system consisting of a UV/VIS detector (SDP-20AV), degasser (DGU-20A), and an autosampler (SIL-HTA). Separation was achieved on an analytic column [Phenomenex Luna C18 (2); 3.0 mol/L, 100 by 4.6 mm]. Full scan spectra, from *m/z* 150 to 700, were obtained in the positive ion mode. The mobile phase consisted of acetonitrile-water with 0.1% acetic acid (50:50, v/v; for 6MAQH) and acetonitrile-water with 0.1% acetic acid (40:60, v/v; for 5MABMA). 6MAQH was detected at 330 nm, whereas 5MABMA was detected at 260 nm. The injection volume was 20 liters and the flow rate was 1 mL/min. Peak areas were monitored and plotted against the concentration. Standard curves were constructed by plotting the peak areas versus diluted concentrations of the stock solutions of the compounds.

Statistical Analysis

Unless otherwise indicated, values in tables and figures are expressed as the mean ± SEM of at least triplicate determinations. Statistical comparisons were made using GraphPad Prism 4.0 software (GraphPad Software, Inc.) by Student's *t* test. A probability value of <0.05 was considered to be significant.

Results

HDACIs Inhibit Growth of Prostate Cancer Cells *In vitro*

To determine whether 6MAQH and 5MABMA, which confer 50% of pan-HDAC activity inhibition at 44 and 200 nmol/L (14), respectively, can effectively suppress cell growth, we treated human prostate cancer PC3 and LNCaP and nonmalignant cells 267-B1 (19) and RWPE-1 (20) with various doses of these inhibitors for 72 h and 96 h. Their effects on cell proliferation were analyzed by MTT assay. The results show that both 6MAQH and 5MABMA abated the growth of prostate cancer cells in a dose-dependent (Fig. 1A and B) and time-dependent manner (Supplementary Fig. S1A and B). After 72 h of exposure, 6MAQH inhibited the proliferation of PC3 and LNCaP by 50% (IC_{50}) at a concentration of 1.95 and 5.15 μmol/L, respectively. At its IC_{50} values, 6MAQH did not exert any significant inhibitory effect on the cell growth of nonmalignant cells. A similar trend was observed for 5MABMA. It impeded the growth of PC3 and LNCaP cells by 50% at 2.1 and 9.8 μmol/L, respectively. Furthermore, prolonged exposure (7 days) of these compounds to normal cells did not render any significant growth-inhibitory effect (<50% growth suppression; Supplementary Fig. S2A and B). The present findings indicate that these structurally related compounds at the concentrations used in this study are more toxic in cancer cells than in nonmalignant prostate cells.

In vitro Metabolic Stability Studies

To evaluate the stability of the compounds, *in vitro* microsomal studies were used. The metabolic stability of 6MAQH and 5MABMA (5 μmol/L) was tested in liver microsomal preparations from humans, dogs, and rats (Fig. 2A and B). Metabolic stability was assessed by monitoring disappearance of the parent compound over the incubation period. The half-lives ($t_{1/2}$) of 6MAQH and 5MABMA in different species are presented in Table 1A. In human and dog microsomes, the half-lives of 6MAQH were determined to be 83 and 72 minutes, respectively, which were longer than that of 5MABMA (68 and 43 minutes, respectively). After 1 h of incubation with liver microsomes, 32% of the initial concentration of 6MAQH remained with the human preparations, but only 22% and 17% remained with the rat and dog preparations (Fig. 2A and B). In addition, 23% and 20% of the initial concentration of 5MABMA remained with the human and rat microsomes, respectively, but only 8% remained with the dog preparations.

In vivo Maximum Tolerated Dose Studies

The *in vivo* efficacy of the compounds was carried out in nude athymic mice. The dose range was based on published HDACIs reports (12, 21). Compound dosages ranging from 0.5 to 400 mg/Kg were administered i.p. in athymic mice and tissue pharmacodynamics was monitored over time. Spleen tissues were removed from animals after 4 h of treatment, based on the highest expression level of acetylated histone H3/H4 in cultured cells following treatment with HDACIs. Western blot analysis revealed that the acetylation of histone H4 was clearly induced and increased in a dose-dependent manner in the spleens of mice after treatment with the compounds. The degree of hyper-acetylation was greater for 5MABMA than 6MAQH at equivalent concentrations (Fig. 3A). Similar results were obtained from different tissues (data not shown). It was noted that 15 minutes after administration of 6MAQH at the highest dose (400 mg/Kg), the mice seemed incapacitated. Nevertheless, this effect was gradually alleviated and the mice were fully recovered within 1 h. The mice behaved normally following administration of 5MABMA at the entire dose range. These studies indicate that 6MAQH and 5MABMA were tolerated in male nude athymic mice.

Antitumor Activity of Mercaptoacetamide-Based HDACIs

To assess the potential of the mercaptoacetamide-based HDACI for antitumor activity *in vivo*, the PC3 cell line,

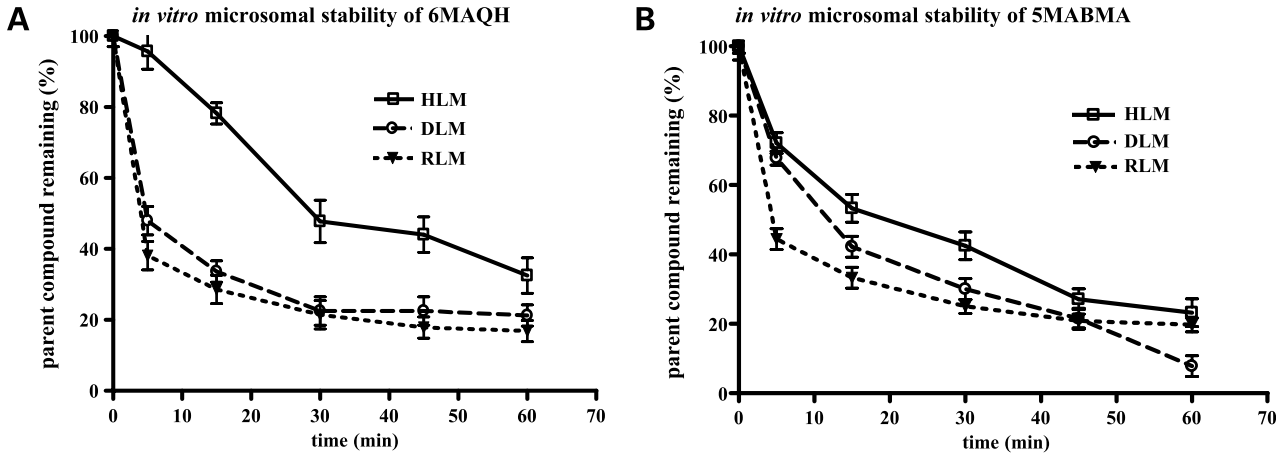

Figure 2. Parent loss of mercaptoacetamide-based HDACI compounds (**A**) 6MAQH and (**B**) 5MABMA following 60-min incubation at 5 μmol/L with human, dog and rat liver microsomes. 6MAQH and 5MABMA were analyzed by LCMS. Three independent experiments were done in triplicates; *points,* mean from a representative triplicate experiment; *bars,* SEM.

Table 1. Stability and pharmacokinetics

A. Comparison of metabolic stability of 6MAQH and 5MABMA, as determined *in vitro* by incubation with human, dogs, and rat liver microsomes

Compound	$t_{1/2}$ (min)		
	Human	Dog	Rat
6MAQH	83	72	66
5MABMA	68	43	70

B. Plasma pharmacokinetic parameters after i.p. administration of 6MAQH and 5MABMA (400 mg/Kg) in nude athymic mice

PK parameters	Compounds	
	6MAQH	5MABMA
C_{max} (μmol/L)	1.81 ± 0.34	1.54 ± 0.26
t_{max} (h)	0.5	0.5
AUC (μmol/L × h)	4.97 ± 0.6	4.23 ± 0.43
$t_{1/2}$ (h)	2.2 ± 0.33	1.98 ± 0.21
CL (L/h)	4.05 ± 0.15	4.87 ± 0.2

NOTE: Microsomal incubations were done in triplicate. Pharmacokinetic (*PK*) parameters are as follows: C_{max}, the maximum plasma concentration; t_{max}, the time to reach maximum plasma concentration; AUC, the area under the compound concentration versus time curve; $t_{1/2}$, the elimination half-life; CL, the clearance.

which tested most sensitive (Fig. 1A and B) for growth inhibition *in vitro*, was used as a tumor xenograft model. To determine a dose response, 6MAQH was administered via i.p. at two dosage levels (0.5 and 5 mg/Kg, daily for 28 days) when tumors reached 150 and 250 mm^3 in volume, respectively. As shown in Supplementary Fig. S3A and B, both dosages effectively reduced the tumor growth in mice with larger sized tumors ($P < 0.01$). The tumor volume barely changed and remained so until the end of the study (28 days). We then examined the efficacy of the low dosage (0.5 mg/Kg) with a shorter treatment schedule. Mice bearing PC3 xenografts were treated with 0.5 mg/Kg *via* daily i.p. administration for 2 weeks (5 days/week). A daily dose of 0.5 mg/Kg was selected as the minimum dose, which manifested pronounced induction of acetylation of histone H4 *in vivo* (Fig. 3A). As shown in Fig. 3B, although the tumor growth rate in 6MAQH- or 5MABMA-treated mice were similar, both were significantly lower than in control-treated mice ($P < 0.01$). The inhibitory effects of 6MAQH and 5MABMA on tumor growth were sustained until the termination of the experiments (60 days). No mortality or body weight loss was detected in mice receiving 6MAQH or 5MABMA, indicating that at the dose tested, these compounds had little or no toxicity (data not shown).

In vivo Pharmacokinetic-Pharmacodynamic Studies

We assessed the pharmacokinetics of 6MAQH and 5MABMA at the maximum tolerated dose (400 mg/Kg) to evaluate *in vivo* exposure. Plasma concentrations were monitored over a 6-hour time period. Figure 4A illustrates the comparison of the plasma concentration versus time curves of the compounds following i.p. administration. Time-dependent plasma accumulation of 6MAQH and 5MABMA were detected. Peak plasma levels were observed at 0.5 h after administration of the compounds. Table 1B summarizes the pharmacokinetic variables. Based on these data, the C_{max} of 6MAQH and 5MABMA were calculated to be 1.81 ± 0.34 and 1.54 ± 0.26 μmol/L and the AUC was 4.97 ± 0.6 and 4.23 ± 0.43 μmol/L × h. The results revealed that the clearance rates for compounds 6MAQH and 5MABMA were 4.05 ± 0.15 and 4.87 ± 0.2 L/h, whereas the half-lives were calculated to be 2.2 ± 0.33 and 1.98 ± 0.21 h, respectively.

Notably, the pharmacokinetic profiles of the compounds in circulation are in agreement with the levels of histone acetylation in tissues. Brain and liver tissues were recovered at 0, 0.5, 1, 2, 4, and 6 h posttreatment, and protein was isolated for Western blot analysis. Both HDACIs elicited a striking accretion in the acetylation of histone H4 in the brain and liver tissues compared with the control (Fig. 4B). At 0.5 h post-dose, the maximum increase in the levels of acetylated histone H4 correlates significantly with peak levels of 6MAQH and 5MABMA in plasma (Fig. 4A). Acetylation of histone H4 remained elevated, relative to the control, for at least 6 h after administration of the compounds. The data suggest that 6MAQH and 5MABMA had sufficient *in vivo* exposure when dosed by the i.p. method of administration.

Discussion

Inhibitors of HDACs are a new class of promising anticancer agents that inhibit tumor growth of a range of transformed cells both *in vitro* and *in vivo* and show very low toxicity toward normal cells (22, 23). The antitumor effect of HDACIs seems to arise from the accumulation of acetylated histones in cells, which in turn regulate chromatin structure and transcription of target genes (24).

Several reports have correlated the hydroxamate group with unfavorable pharmacokinetic properties as well as short *in vivo* half-lives (25, 26). For example, a structurally novel cinnamic hydroxamic acid analogue, Panobinostat (LBH589), has low oral bioavailability in rodents, which is

markedly higher in dogs than that in rats (6% and 33–50%, respectively; Novartis Pharmaceuticals, data on file). Of synthetic benzamide derivatives, Entinostat (MS-275) exhibits the half-life of 36 h in the patient, far longer than predicted in animal studies, whereas the AUC did not increase proportionally with dose (27). CI-994 has shown efficacy in solid tumors in murine models but did not inhibit HDAC directly. There are reports of novel nonhydroxamate sulfonamide anilides similar in structure to MS-275 that have shown lower toxicity and comparable antiproliferative activity (28, 29). Therefore, the current research has focused on the development of novel compounds, which may have a better HDAC inhibitory profile and lower toxicity compared with existing parent compounds.

Recently, the thiol group has been designated as a good replacement for the hydroxamic acid and thiol derivatives have been documented to inhibit zinc dependent enzymes, which includes HDAC enzymes, matrix metalloproteinases, and angiotensin-converting enzymes (30–33). Our mercaptoacetamide-based HDACIs (6MAQH and 5MABMA) have proven to inhibit pan-HDAC activity at nanomolar concentrations (14, 34) and protect *in vitro* cortical neurons from oxidative stress-mediated death (35). Another study revealed that mercaptoacetamide-based HDACIs attenuated microglia inflammatory response and decreased neuronal degeneration in the hippocampus in rats following traumatic brain injury (36).

Ours is the first report describing the comparative *in vitro* and *in vivo* properties of two thiol compounds with particular reference to pharmacokinetic-pharmacodynamic relationships and how this information may be used to support the development of mercaptoacetamide-based HDACIs. First, these HDACIs preferentially sensitize prostate cancer cells (PC3 and LNCaP) at concentrations that exert minimal effect on the growth of nonmalignant prostate epithelial cells (RWPE-1 and 267-B1). Second, *in vitro* liver microsomal studies exclude any contribution of HDACI-related metabolites to the cytotoxic effects, supporting the stability of these structurally related compounds with limited metabolic degradation. On these bases, and in light of two recent studies demonstrating the protective role of mercaptoacetamide-based HDACIs (35, 36) in normal cells, we hypothesize that the compounds manifest selectivity toward cancer cells.

Furthermore, *in vivo* results show that both mercaptoacetamide-based HDACIs significantly reduced the growth of PC3 tumor xenografts in athymic nude mice at a dose (0.5 mg/Kg) that causes no apparent sign or symptom of toxicity in mice and exhibit favorable pharmacokinetic-pharmacodynamic relationships *in vivo*. With regard to

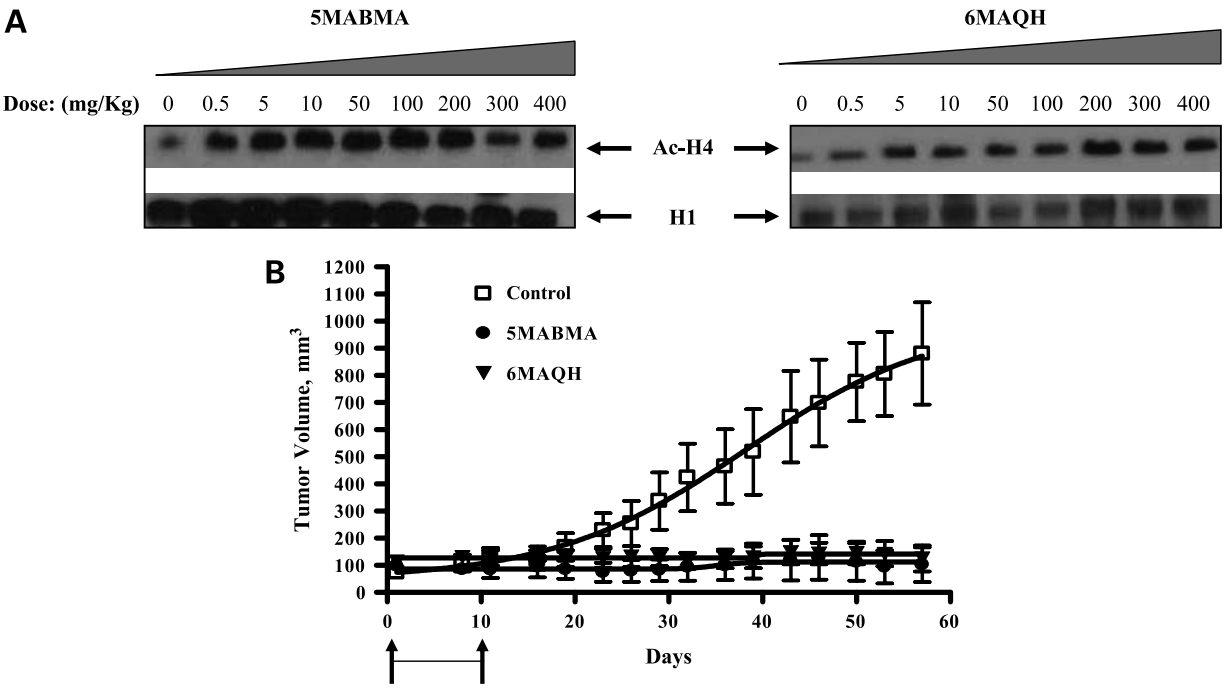

Figure 3. **A,** 6MAQH and 5MABMA (0.5–400 mg/Kg) were administered to athymic nude mice by the i.p. route. Spleen tissues were removed 4 h after treatment, and protein was subjected to Western blot assay using antibodies against acetylated histone H4 (*Ac-H4*). Each lane was loaded with 20 μg protein and the membrane was reprobed with histone H1 to ensure equal loading. **B,** the effects of i.p. administration of mercaptoacetamide HDACIs on the growth of human prostate PC3 tumor xenografts. Male nude athymic mice bearing established PC3 xenografts were randomized into control and treatment groups ($n = 10$ mice/group). Treatment groups received i.p. a single dose of 0.5 mg/Kg of 6MAQH and 5MABMA daily, 5 d/wk for 2 wk. *Arrows,* the duration of treatment. The tumor volumes were monitored up to 60 d. The percentage change in tumor volume (*V*) from baseline was used to assess the response to treatment. *Points,* mean tumor volumes are shown at the times that tumor measurements were made; *bars,* SEM. The tumor growth rate in 6MAQH or 5MABMA-treated mice was significantly lower than in control-treated mice (Student's *t* test, $P < 0.01$) but were not different from each other.

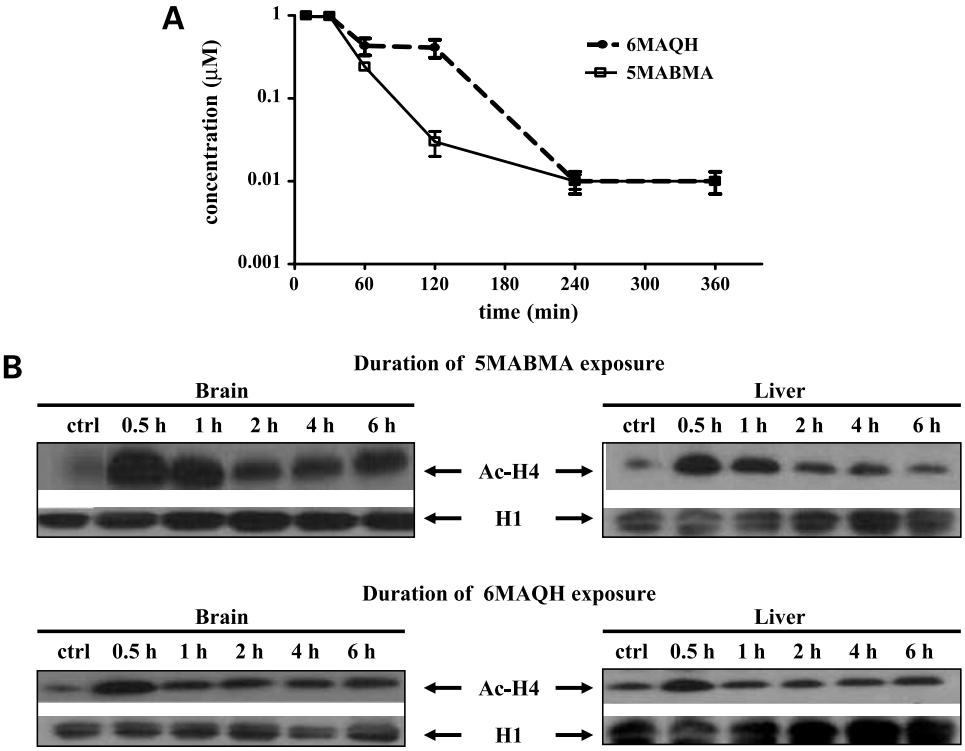

Figure 4. **A,** comparison of plasma concentrations versus time profiles of 6MAQH and 5MABMA following i.p. administration at 400 mg/Kg to nude athymic mice. Plasma samples were collected at various times up to 6 h. 6MAQH and 5MABMA were analyzed by LCMS. *Points,* mean of three animals per time point for each compound; *bars,* SEM. Pharmacokinetic parameters are presented in Table 1B. **B,** tissues (brain, liver) were removed at 0, 0.5, 1, 2, 4, and 6 h following i.p. administration of the compounds. Lysates of the tissues were subjected to Western blotting using an antibody against acetylated H4 histone (*Ac-H4*). Each lane was loaded with 20 μg protein and membrane was reprobed with histone H1 to ensure equal loading.

plasma pharmacokinetic variables (Table 1B), 6MAQH had the highest plasma concentration (C_{max}) of 1.81 ± 0.34 μmol/L and exhibited the longest half-life of 2.2 ± 0.33 h and the slowest clearance of 4.05 ± 0.15 L/h. The plasma C_{max} (1.81 ± 0.34 μmol/L) value of 6MAQH obtained with the 400 mg/Kg dose is very close to the *in vitro* IC_{50} value (1.95 μmol/L). The *in vivo* antitumor effect seen with the low dose of 6MAQH (0.5 mg/Kg) suggests potential of antitumor efficacy with reduced systemic toxicity. The accumulation of 6MAQH in tumors may also account for its selective antiproliferation effects on cancer cells (PC3 and LNCAP) as opposed to normal cells (RWPE-1 and 267-B1). In an earlier study (13), we documented that 6MAQH (coded as W2) exhibited higher lipophilicity value than SAHA with log *D* of 2.64 and 1.46, respectively. This chemical property may facilitate the penetration and retention of 6MAQH in tumor cells. Similarly, 5MABMA revealed C_{max} of 1.54 ± 0.26 μmol/L and half-life of 1.98 ± 0.21 h and clearance rate of 4.87 ± 0.2 L/h. These observations are consistent with previous data demonstrating that both mercaptoacetamide HDACIs manifested long plasma half-lives *in vitro* and were more stable compared with SAHA (13). Our findings indicate that mercaptoacetamide-based HDACIs remain in the plasma at high levels for a long period of time and this suggests that they can have prolonged effects *in vivo*, which may in turn permit a reduction in dosage frequency. Moreover, this was accompanied by an increase in the levels of acetylated histone H4 in tissues, indicating that both compounds reach their target in sufficient concentrations to suppress HDAC actions *in vivo*.

These data show that mercaptoacetamide-based HDACIs target prostate cancer cells effectively, as evidenced by growth inhibition *in vitro* and tumor regression *in vivo*. Furthermore, pharmacokinetic-pharmacodynamic results support their potential in the treatment of prostate cancer.

Disclosure of Potential Conflicts of Interest

No potential conflicts of interest were disclosed.

Acknowledgments

We thank Gene Therapy Pharmaceuticals for preparing the compound.

References

1. Gronberg H. Prostate cancer epidemiology. Lancet 2003;361:859–64.
2. Signoretti S, Loda M. Prostate stem cells: from development to cancer. Semin Cancer Biol 2007;17:219–24.
3. Marks PA, Rifkind RA, Richon VM, Breslow R, Miller T, Kelly WK. Histone deacetylases and cancer: causes and therapy. Nat Rev Cancer 2001;1:194–202.
4. Karagiannis TC, El-Osta A. The paradox of histone deacetylase inhibitor mediated modulation of cellular responses to radiation. Cell Cycle 2006;5:288–95.

5. Johnstone RW. Histone-deacetylase inhibitors: novel drugs for the treatment of cancer. Nat Rev Drug Discov 2002;1:287–99.

6. McLaughlin F, La Thangue NB. Histone deacetylase inhibitors open new doors in cancer therapy. Biochem Pharmacol 2004;68:1139–44.

7. Minucci S, Pelicci PG. Histone deacetylase inhibitors and the promise of epigenetic (and more) treatments for cancer. Nat Rev Cancer 2006;6: 38–51.

8. Munster PN, Troso-Sandoval T, Rosen N, Rifkind R, Marks PA, Richon VM. The histone deacetylase inhibitor suberoylanilide hydroxamic acid induces differentiation of human breast cancer cells. Cancer Res 2001;61: 8492–7.

9. Carducci MA, Gilbert J, Bowling MK, et al. A phase I clinical and pharmacological evaluation of sodium phenylbutyrate on 120-h infusion schedule. Clin Cancer Res 2001;7:3047–55.

10. Ryan QC, Headlee D, Acharya M, et al. Phase I and pharmacokinetic study of MS-275, a histone deacetylase inhibitor, in patients with advanced and refractory solid tumors or lymphoma. J Clin Oncol 2005;23: 3912–22.

11. Byrd JC, Marcucci G, Parthun MR, et al. A phase I and pharmacodynamic study of depsipeptide (FK228) in chronic lymphocytic leukemia and acute myeloid leukemia. Blood 2005;105:959–67.

12. Kelly WK, O'Connor OA, Krug ML, et al. Phase I study of an oral histone deacetylase inhibitor, suberoylanilide hydroxamic acid, in patients with advanced cancer. J Clin Oncol 2005;23:3923–31.

13. Konsoula R, Jung M. *In vitro* plasma stability, permeability and solubility of mercaptoacetamide histone deacetylase inhibitors. Int J Pharm 2008;361:19–25.

14. Chen B, Petukhov PA, Jung M, et al. Chemistry and biology of mercaptoacetamides as novel histone deacetylase inhibitors. Bioorg Med Chem Lett 2005;15:1389–92.

15. Mosmann T. Rapid colorimetric assay for cellular growth and survival: application to proliferation and cytotoxicity assays. J Immunol Methods 1983;65:55–63.

16. Konsoula R, Barile FA. Correlation of *in vitro* cytotoxicity with paracellular permeability in Caco-2 cells. Toxicol In Vitro 2005;19:675–84.

17. Konsoula R, Barile FA. Correlation of *in vitro* cytotoxicity with paracellular permeability in mortal rat intestinal cells. J Pharmacol Toxicol Methods 2007;55:176–83.

18. Konsoula Z, Jung M. Involvement of p-glycoprotein and multidrug resistance associated protein 1 on the transepithelial transport of a mercaptoacetamide-based histone-deacetylase inhibitor in caco-2 cells. Biol Pharm Bull 2009;32:74–8.

19. Kaighn ME, Reddel RR, Lechner JF, et al. Transformation of human neonatal prostate epithelial cells by strontium phosphate transfection with a plasmid containing SV40 early region genes. Cancer Res 1989;49: 3050–6.

20. Webber MM, Bello D, Kleinman HK, Wartinger DD, Williams DE, Rhim JS. Prostate specific antigen and androgen receptor induction and characterization of an immortalized adult and human prostatic epithelial cell line. Carcinogenesis 1996;17:1641–6.

21. Ramalingam SS, Parise RA, Ramananthan RK, et al. Phase I and pharmacokinetic study of vorinostat, a histone deacetylase inhibitor, in combination with carboplatin and paclitaxel for advanced solid malignancies. Clin Cancer Res 2007;13:3606–10.

22. Ishdorj G, Graham BA, Hu X, et al. Lysophosphatidic acid protects cancer cells from histone deacetylase (HDAC) inhibitor-induced apoptosis through activation of HDAC. J Biol Chem 2008;283:16818–29.

23. Secrist JP, Zhou X, Richon VM. HDAC inhibitors for the treatment of cancer. Curr Opin Investig Drugs 2003;4:1422–7.

24. Mühlethaler-Mottet A, Flahaut M, Bourloud KB, et al. Histone deacetylase inhibitors strongly sensitise neuroblastoma cells to TRAIL-induced apoptosis by a caspases-dependent increase of the pro- to anti-apoptotic proteins ratio. BMC Cancer 2006;6:214–27.

25. Mulder GJ, Meerman JH. Sulfation and glucuronidation as competing pathways in the metabolism of hydroxamic acids: the role of *N, O*-sulfonation in chemical carcinogenesis of aromatic amines. Environ Health Perspect 1983;49:27–32.

26. Suzuki T, Matsura A, Kouketsu A, Nakagawa H, Miyata N. Identification of a potent non-hydroxamate histone deacetylase inhibitor by mechanism-based drug design. Bioorg Med Chem Lett 2005;15:331–5.

27. Prince HM, Bishton MJ, Simon J, Harrison SJ. Clinical studies of histone deacetylase inhibitors. Clin Cancer Res 2009;15:3958–69.

28. Fournel M, Trachy-Bourget MC, Yan PT, et al. Sulfonamide anilides, a novel class of histone deacetylase inhibitors, are antiproliferative against human tumors. Cancer Res 2002;62:4325–30.

29. Bouchain G, Leit S, Frechette S, et al. Development of potential antitumor agents. Synthesis and biological evaluation of a new set of sulfonamide derivatives as histone deacetylase inhibitors. J Med Chem 2003; 46:820–830.

30. Jung M, Brosch G, Kolle D, Scherf H, Gerhauser C, Loidl P. Amide analogues of Trichostatin A as inhibitors of histone deacetylase and inducers of terminal cell differentiation. J Med Chem 1999;42: 4669–79.

31. Michaelides MR, Dellaria JF, Gong J, et al. Biaryl ether retro-hydroxamates as potent, long-lived, orally bioavailable MMP inhibitors. Bioorg Med Chem Lett 2001;11:1553–6.

32. Remiszewski SW, Sambucetti LC, Atadja P, et al. Inhibitors of human histone deacetylase: synthesis and enzyme and cellular activity of straight chain hydroxamates. J Med Chem 2002;45:753–7.

33. Suzuki T, Kouketsu A, Matsuura A, et al. Thiol-based SAHA analogues as potent histone deacetylase inhibitors. Bioorg Med Chem Lett 2004;14:3313–7.

34. Anandan SK, Ward JS, Brokx RD, Bray MR, Patel DV, Xiao XX. Mercaptoamide-based non-hydroxamic acid type histone deacetylase inhibitors. Bioorg Med Chem Lett 2005;15:1969–72.

35. Kozikowski AP, Chen Y, Gaysin A, et al. Functional differences in epigenetic modulators superiority of mercaptoacetamide-based histone deacetylase inhibitors relative to hydroxamates in cortical neuron neuroprotection studies. J Med Chem 2007;50:3054–61.

36. Zhang B, West EJ, Van KC, et al. HDAC inhibitor increases histone H3 acetylation and reduces microglia inflammatory response following traumatic brain injury in rats. Brain Res 2008;1226:181–91.